The genomic complexity of a large inversion in great tits

Vinicius H. da Silva[1,2,3], Veronika N. Laine[4], Mirte Bosse[1], Lewis G. Spurgin[5], Martijn F. L. Derks[1] Kees van Oers[2], Bert Dibbits[1], Jon Slate[6], Richard P.M.A Crooijmans[1], Marcel E. Visser[1,2], Martien A. M. Groenen[1]*

[1]*Animal Breeding and Genomics, Wageningen University & Research*

[2]*Department of Animal Ecology, Netherlands Institute of Ecology (NIOO-KNAW)*

[3]*Swedish University of Agricultural Sciences (SLU)*

[4]*Department of Molecular and Cellular Biology, Harvard University*

[5]*School of Biological Sciences, University of East Anglia, Norwich Research Park University of East Anglia*

[6]*Department of Animal and Plant Sciences, The University of Sheffield*

*Author for Correspondence: Martien A. M. Groenen, Wageningen University & Research, Animal Breeding and Genomics.

Droevendaalsesteeg 1

6708 PB Wageningen - The Netherlands

+31 0317486001

martien.groenen@wur.nl

Abstract

Chromosome inversions have clear effects on genome evolution and have been associated with speciation, adaptation and the evolution of the sex chromosomes. In birds, these inversions may play an important role in hybridization of species and disassortative mating. We identified a large (≈64 Mb) inversion polymorphism in the great tit (*Parus major*) that encompasses almost 1,000 genes and more than 90% of Chromosome 1A. The inversion occurs at a low frequency in a set of over 2,300 genotyped great tits in the Netherlands with only 5% of the birds being heterozygous for the inversion. In an additional analysis of 29 resequenced birds from across Europe we found two heterozygotes. The likely inversion breakpoints show considerable genomic complexity, including multiple copy number variable segments. We identified different haplotypes for the inversion, which differ in the degree of recombination in the center of the chromosome. Overall, this remarkable genetic variant is widespread among distinct great tit populations and future studies of the inversion haplotype, including how it affects the fitness of carriers, may help to understand the mechanisms that maintain it.

Key Words: songbird, structural variation, CNVs, *Parus major*

Introduction

Inversions are structural intra-chromosomal mutations resulting in the reversal of gene/sequence order. Chromosomal inversions represent an important class of polymorphism that are of particular interest in evolutionary studies (Hoffmann and Rieseberg, 2008; Kirkpatrick, 2010). Numerous studies have shown inversions to be important factors in speciation and adaptation (reviewed in Hoffmann and Rieseberg 2008). Studies of hominin evolution indicate a role of inversions in the process, with more than one thousand inversions arising in both the human and chimpanzee lineages since they shared a common ancestor (Hellen, 2015). Red fire ants (*Solenopsis invicta*) provide an interesting example of how inversions can promote adaptation; whether or not ant colonies contain a single queen or multiple queens depends on which inversion genotype is present the colony. The two social forms are genetically isolated (Keller and Ross, 1998; Wang et al., 2013). In passerines, inversions are significantly more common in clades with more sympatric species, which suggests that inversions may often evolve or be maintained because they suppress recombination between the genomes of hybridizing species (Hooper and Price, 2017). In both the white-throated sparrow (*Zonotrichia albicollis*) and the ruff (*Calidris pugnax*), morphs with different sexual behaviours are determined by inversions (Küpper et al., 2015; Lamichhaney et al., 2016; Tuttle et al., 2016). The inversion in the white-throated sparrow is very large, harboring ≈1,000 genes, and lethal in homozygous state (Tuttle et al., 2016).

To explain how inversions are maintained in a population it is important to understand the different mechanisms underlying selection on inversions. There can be meiotic drive if the

inversion harbors alleles that alter segregation distortion (Kirkpatrick, 2006). Selective advantages can also occur when an inversion affects the expression of advantageous genes located within or closely linked to the inversion (Puig et al., 2004). The effect of the inversion on gene expression is well documented in red fire ants (Huang et al., 2018; Lucas et al., 2015; Nipitwattanaphon et al., 2013; Wang et al., 2008, 2013). In this species, gene expression differences between the monogyne and polygyne social forms are greatest in the inversion, suggesting that the inversion plays a key role in morphological and behavioural differences between the two forms. In addition, selective advantages of an inversion can be the result of recombination disruption in heterozygotes, which can preserve advantageous alleles. Moreover, reduced crossing-over within the inversion is associated with higher recombination rate elsewhere in the genome (Stevison et al., 2011), which in turn can modulate selection (McGaugh et al., 2012).

In many cases, recombination is suppressed between an inverted haplotype and the wild haplotype (Butlin, 2005; Hoffmann and Rieseberg, 2008; Kirkpatrick, 2006, 2010). As a result of this lack of recombination in heterozygous inversion carriers, strong linkage disequilibrium between loci within the inverted region can rapidly build up. Although the lack of recombination can maintain advantageous variants without disruption throughout generations (i.e. supergenes, reviewed in Thompson and Jiggins 2014), there are also possible costs associated with the suppression of recombination. Each of the inversion haplotypes will behave as a single heritable entity that can help to retain certain alleles in the population even when they are subject to purifying selection (i.e. deleterious recessive alleles can be maintained if they are found within

inversion polymorphisms by a "hitchhiking" effect, Kirkpatrick 2006). As a consequence, deleterious recessive alleles can accumulate in regions of low recombination, such as an inversion, as they are no longer effectively removed by purifying selection. Moreover, throughout evolution an inversion becomes structurally more complex than the non-inverted counterpart and often experiences a degenerative process (Tuttle et al., 2016). This degenerative process has been reported to be associated with a size increase in young supergenes (Stolle et al., 2018). In general, an increase in the number of gene copies can alter trans- and cis- gene expression, which might generate novel phenotypic variation (Geistlinger et al., 2018).

Inversions may harbor complex genomic rearrangements at their breakpoints (Calvete et al., 2012), given that inversion breakpoints are more likely to happen at complex parts of a chromosome (Carvalho and Lupski, 2016). Apart from changing the gene order, inversions also often involve gene duplications that can lead to genetic novelty and subsequent adaptation (Furuta et al., 2011). In mosquitoes from the species complex *Anopheles gambiae*, haplotypes involving structural rearrangements at the breakpoint of a paracentric inversion have shed light on the origin and evolution of their malaria vectorial capacity (Sharakhov et al., 2006). The presence of repetitive regions at inversion breakpoints is recurrent and in fact both inversions and repetitive regions can share the same mechanism of formation, such as non-allelic homologous recombination (NAHR) (Carvalho and Lupski, 2016; Kehrer-Sawatzki and Cooper, 2008). Understanding structural variations linked to inversion breakpoints may help to clarify the possible functionality and evolutionary history of inversions.

Genetic markers like SNPs and sequence data can be used to identify inversions polymorphism given the distinct population genetic structure caused by LD patterns within inversions. Thus, methods that are based on principal components analysis (PCA) can detect the unusual genetic structure of inversions (Ma and Amos, 2012). In this study, we describe a 64.2 Mb putative inversion on Chromosome 1A in great tits (*Parus major*), a widely studied songbird in ecology and evolution (Husby et al., 2011; Kvist et al., 2003; Visser et al., 1998) with a broad range of genomic resources such as a high density SNP array (Kim et al., 2018), reference genome and methylome analysis (Laine et al., 2016) as well as copy number variation (CNV) maps (da Silva et al., 2018; Kim et al., 2018).

Materials and Methods

Population description, genotyping and sequencing. A total of 2,322 great tits were genotyped using a custom made Affymetrix great tit 650K SNP chip (Kim et al., 2018) at Edinburgh Genomics (Edinburgh, United Kingdom). SNP calling was done following the Affymetrix best practices workflow by using the Axiom Analysis Suite 1.1. After sample filtering, 26 birds with dish quality control (DQC, Nicolazzi et al. (2014)) <0.82 and SNP call rate <95% were discarded. SNPs with minor allele frequency (MAF) <1% and call rate <95% were removed. Only autosomes were used in this study. After filtering, 2,296 birds and 514,799 SNPs were kept for subsequent analysis. The genotyped birds were from our long-term study populations on the Veluwe area near Arnhem, the Netherlands (52°02 N, 5°50 E). More information regarding the origin of the birds and the *in vitro* DNA procedures are described by da Silva et al. (da Silva et al., 2018). The raw genotype

data used in this study was submitted to GEO (GSE105131). Filtered genotypes and the source code to perform all analyses described below are available at Open Science Framework (OSF, `https://osf.io/t6gnd/?view_only=821507ec135b44778d8b80254c24633b`).

In addition to the birds genotyped on the SNP chip, we also used sequence data from 29 birds (10 from the Wytham Woods population in Oxford (UK), 19 birds sampled from 15 other European populations). Each bird was sequenced at an average depth of around 10x using paired-end sequencing libraries. Details of sequencing analysis, as well as information regarding the origin and sample quality of each bird are provided elsewhere (Laine et al., 2016).

Identification and characterization of a large inversion on Chromosome 1A. Population structure between SNP-typed individuals was explored using a principal components analysis (PCA) approach, previously applied for the study of inversions (Ma and Amos, 2012), using the `snpgdsPCA` function in SNPRelate R/Bioconductor package (v. 1.10.2) (Patterson et al., 2006; Zheng et al., 2012). Each autosome was analysed separately.

Following PCA, we estimated the fixation index (F_{ST}) in a SNP-wise fashion, using the `Fst` function available in snpStats R/Bioconductor package (v. 1.26.0) (Clayton, 2015) to compare birds in different clusters identified by visual inspection (i.e. subpopulations) of PCA plots. As SNP heterozygosity is expected to be higher within the inversion in carriers (i.e. birds with two different inversion haplotypes), the ratio of heterozygous birds (i.e "AB") for each SNP was assigned within each subpopulation. The SNP-wise F_{ST} and heterozygosity values were used to define the likely breakpoints of the inversion.

Pairwise D' values, (Lewontin and Kojima, 1960) using all birds, were calculated to assess linkage disequilibrium patterns on Chromosome 1A. To aid visualization of the patterns revealed by the SNP data, SNPs were pruned to retain loci with MAF >0.4 and an LD threshold of 0.05 (using genomic windows with a maximum size of 500 kb). Pruning was performed with the `snpgdsLDpruning` and `snpgdsLDMat` functions within the SNPRelate R/Bioconductor package (v. 1.10.2) (Zheng et al., 2012). A total of 214 SNPs was retained and used in the LD analysis plot. We produced a graphical representation of the LD map using the `LDheatmap` function from the LDheatmap R package (v. 0.99-2) (Shin et al., 2006). The function used to infer LD in this study makes use of the expectation-maximization (EM) algorithm (Excoffier and Slatkin, 1995), which is able to infer LD from unphased data. In addition, the R^2 (Zaykin et al., 2008) estimator was used for comparison with results from D' because each estimator may respond differently to low frequency alleles (Wray, 2005).

Inference of structural complexity at Chromosome 1A. We used copy number variation (CNV) data obtained from SNP intensity information from the same great tit population in the Netherlands, as described previously (da Silva et al., 2018), to evaluate if certain CNVs are associated with normal/inverted phases. Moreover, we identified CNVs in the 29 resequenced birds from different European populations (Laine et al., 2016)). First, we used the $.bam$ file of each sample, containing reads mapped onto the reference genome build 1.1 using BWA (Li and Durbin, 2009), to extract map locations with samtools (Li et al., 2009) as described in CNV-seq manual (Xie and Tammi, 2009). CNVs were called with the default parameters of CNV-seq (Xie and Tammi, 2009). CNV-seq uses coverage information to calculate a $\log_2$ transformed ratio between the subject samples

(inv-norm only, because inv-inv birds were absent from the dataset) and wild-type samples (norm-norm). A positive ratio is associated with copy-number gain (duplication), while a negative ratio is associated with copy-number loss (deletion).

In addition, we used Lumpy (Layer et al., 2014) with default parameters, incorporated in the speedseq pipeline (Chiang et al., 2015) to predict the exact breakpoints of the CNV events and to predict inversion events from sequence data. Information from split and discordant mapped reads was used to describe the structure of a CNV complex in one of the inversion breakpoints (details in the supplementary section 3.4- Patterns in split reads supporting the CNV complex).

Inversion detection by PCR-RFLP. As genotyping with SNP arrays can be time consuming and expensive, we designed an alternative method to type the Chromosome 1A inversion, based on a PCR followed by a restriction enzyme digestion (PCR-RFLP). For this, we used the SNP with the second highest F_{ST} value (i.e. AX-100689781) because it almost perfectly captures the inversion (99.32% of the inv-norm birds have AB genotype and 98.95% of the norm-norm birds have the AA genotype). The SNP with the highest F_{ST} value did not allow distinguishable fingerprints *in silico* because there are no restriction enzymes which differentially cut the two alleles. Instead, we choose SNP AX-100689781 which is located close to the downstream breakpoint of the inversion, at position 65,878,384 in the great tit genome build 1.1 (Laine et al., 2016) (details in the supplementary section primer design and enzyme search). This SNP is located within the first intron of the gene *PIK3C2G*. We genotyped 42 birds by PCR-RFLP which had also been genotyped with the SNP-chip.

For each PCR-RFLP reaction we used 6μl of DNA (10ng/μl). The PCR was performed with OneTaq 2X mastermix (New England Biolabs) and 1μl of primermix (primer sequences are given in the supplementary section primer design and enzyme search). The PCR program had steps of: 95°C for 5 min, 34 cycles of 95°C for 30 seconds, 55°C for 45 seconds, 72°C for 90 seconds and a final elongation step of 72°C for 10 min. The digestion reaction was done for 5 hrs at 37°C using 3μl of the PCR product, 0.4μl of the enzyme $SspI$ (10U/μl, New England Biolabs), 1μl of the $SspI$ buffer 10X and 5.6μl of sterile deionized water (MQ). The PCR-RFLP was analyzed on a 3% agarose gel. The restriction fragments were checked on the Geldoc XR+(Biorad) gel documentation system with the software Image Lab (v. 5.2.1).

Results

Population structure for Chromosome 1A reveals a large inversion. We found a large putative inversion on Chromosome 1A. Based on visual inspection of the principal component analysis (PCA) (Patterson et al., 2006), we classified the clustering patterns separately for each autosome in the great tit genome (Sup Fig 1). Plots for whole chromosomes may reveal obvious substructure if the inversion is relatively large. Although additional chromosomes display some population structure (e.g. chromosomes 5 and 7, Figure S1 and S2), the variation within PCA clusters is greater, and the F_{ST} values across these chromosomes less conclusive, relative to the patterns seen on Chromosome 1A. Moreover, this unusual PCA pattern, which was most likely reflecting an inversion, was briefly reported elsewhere (Bosse et al., 2017). Therefore, the remainder of this paper considers the likely inversion polymorphism on Chromosome 1A.

Chromosome 1A displayed clear population structure for the first eigenvector (Figure 1a, First and Second eigenvectors explain 2.28 and 0.50% of the variance, respectively), with two subpopulations that are genetically distinct. The larger subpopulation comprises 2,179 birds and the smaller one contains only 117. Among these 117 birds, ten display intermediate values in Eigenvector One. Analysis of the genotypes of these ten birds indicates that they are carrying a distinct copy of the inversion that is derived, possibly by gene conversion, from the most common inversion haplotype (i.e the ten being heterozygotes and the remainder being homozygous for the inversion haplotype). The genotypes and LD patterns in the center of the inversion are discussed in detail in a subsequent section (i.e. Linkage-disequilibrium and haplotypes across the inversion).

We obtained high F_{ST} values between the two PCA plot subpopulations across almost the whole of Chromosome 1A except for the most distal SNPs on the chromosome (Figure 1b). The heterozygosity level in each of these subpopulations across Chromosome 1A is also strikingly different (Figure 1c). The heterozygosity level for the smaller subpopulation is greater than for the larger subpopulation, except for markers close to the telomeres. This suggests that the smaller subpopulation contains birds heterozygous for the inversion polymorphism. The heterozygosity patterns are consistent with the pattern shown by the F_{ST} analysis, in terms of where the inversion is located on the chromosome. In addition, the F_{ST} values of the SNPs located on Chromosome 1A have a significantly different distribution than SNPs in the rest of the genome (Wilcoxon rank sum test with continuity correction *p*-value ≈ 0.0002).

The PCA, F_{ST} and heterozygosity results support the existence of a pericentric inversion

in the smaller PCA subpopulation (117 birds). This putative inversion comprises ≈90% of the length of the chromosome (≈64.2 Mb) and is present only in heterozygous state in this great tit population (given the PCA clustering in addition to the high levels of heterozygosity of the SNPs at Chromosome 1A in inv-norm birds, Figure 1a-c).

Linkage-disequilibrium and haplotypes across the inversion. We used the unphased SNP genotypes from all birds to characterize linkage-disequilibrium (LD) across Chromosome 1A by calculating D' (Lewontin, 1964). As expected for regions with low recombination, a large LD block which overlaps the whole inversion was identified (Figure 2a). This LD block is not present in norm-norm birds (Figure 2b), suggesting that recombination is only restricted in birds heterozygous for the inversion. On the other hand, when R^2 is used as a measure of LD inference, an LD block is only observed in the middle of the chromosome (from position ≈24.6 to 48.8 Mb, Figure 2c). This R^2 LD block overlaps the region that causes the two distinct genotype distributions among the 117 inv-norm birds (Figure 2d).

Initial results show that phasing procedures, such as BEAGLE, fail in inv-norm birds (data not shown). Consequently, these wrongly phased alleles could lead to wrong conclusions about inversion sequences. Therefore, a detailed analysis of genetic diversity within the different inversion haplotypes was not possible. Instead, we used genotype information to explore putative inversion haplotypes. In the center of the inversion (a 20-55 Mb window was used, which is a 5 Mb up- and downstream extension of the LD block in the center due to uncertainty over the precise breakpoint locations), the genotype frequencies (i.e. the ratio of genotypes “AA”, “AB”

and “BB”, where “A” is the major and “B” the minor allele in the general population) is substantially different between the ≈10% of the inv-norm birds (ten birds, Figure S5) and the remainder of the inv-norm birds. The number of “AA” SNP genotypes (i.e. homozygous for the major allele, which is rare in the inversion) in these ten inv-norm birds that differ from the others is greater than in the other inv-norm birds. A total of 107 birds (91.4%) have between 4 and 30 (mean = 11.61, standard deviation = 4.95) SNPs with genotype “AA” while the remaining 10 birds have substantially more “AA” genotypes (range = 146-1,382; mean = 892.4; standard deviation = 394.2; Figure 3). To a certain extent the ten birds with distinct haplotypes can also be distinguished from the other inv-norm birds, by the PCA analysis due to their intermediate values in eigenvector one (0.053 to 0.076). These ten birds are from four different areas in Netherlands (2 birds from Buunderkamp; 3 birds from Westerheide; 2 birds from Roekelse Bos; 2 birds from Hoge Veluwe and one birds from an unknown location).

Complex genomic structure at the inversion breakpoint. Inversion breakpoints can provide insight in the evolutionary history of the inversion (Sharakhov et al., 2006). The downstream breakpoint of the Chromosome 1A inversion harbors a previously identified CNV region, 2802, located at position 64.83-67.67 Mb (Figure 4a, da Silva et al. 2018). Of all 2,296 birds analyzed for the inversion, 2,021 were also previously analyzed for copy number variations. This includes 1,921 birds classified as norm-norm and 100 as inv-norm. Among the norm-norm birds, 217 harbor CNVs at the downstream inversion breakpoint (11.29%) whereas 1,704 have two copies as expected in the diploid state. By contrast, 96% of the inv-norm birds have an individual CNV call mapped at the CNVR 2802. At this CNVR, 94.8% of all individual CNV calls are gains.

Inversion detection with PCR-RFLP. We looked for SNPs with the highest F_{ST} possible, which concomitantly allowed different DNA fingerprints of their SNP genotypes to be obtained by restriction digest. For the SNP with the second highest F_{ST} value (Figure 4b), "AA" and "AB" genotypes (i.e. associated with norm-norm and inv-norm karyotypes, respectively), our genotype assay produced two distinct *in silico* profiles when the PCR fragments were digested by the enzyme *SspI* (Figure 4d, represented by the black bars). The SNP is located in the first intron of the *PIK3C2G* gene. In a diploid region, we would expect a profile with four bands (i.e. "AB") in an inv-norm bird whereas a profile with two bands (i.e. "AA") would be norm-norm. However, as the SNP is placed in a repetitive region (i.e. containing a CNVR and segmental duplications), the obtained profiles are more complex. We obtained instead four different profiles, which differ in the intensity in each of the four possible fragments (Figure 4d). Profile B3 was only identified in inv-norm samples whereas the profiles B1, B2 and B4 were mostly, but not exclusively observed in norm-norm samples. However, birds with the profile B2, in 90% of the cases, are norm-norm and in 10% inv-norm. Unexpectedly, the profile B4, which shows high heterozygosity as in the inversion, was only identified in two norm-norm birds (0% of confidence, i.e. expected to be found in inv-norm but only found in norm-norm birds).

Assessing breakpoint complexity from sequencing data. We classified 29 birds for the inversion from distinct European populations by whole genome resequencing (Laine et al., 2016) based on the presence of the CNV complex at the breakpoint. A total of 27 birds were classified as norm-norm and two as inv-norm. We used sequencing data from the two inv-norm birds, one from France and another from Belgium, to characterize CNVs across the inversion. At the downstream

breakpoint, we detected a CNV (gain state) in both birds in agreement with the results from the Dutch great tit population, which suggests a high correlation of the inversion with a gain state at the downstream breakpoint (Figure 4c). None of the other 27 resequenced birds without the inversion showed CNVs at this region. The CNVs that we identified in the two inv-norm resequenced birds point to a substantial increase in the number of copies instead of only a single copy gain. The log_2 values from CNV-seq at that region suggest around ten copies in the inverted phase involving three CNVs that are part of the same structural complex (the regions between 65.87-65.90, 67.56-67.58 and 67.64-67.65 Mb, which together comprise ≈50.43 kb). In addition, we identified an increase of around 100 copies in a region upstream to the CNV complex (63.44-63.46 Mb, ≈20 kb), which in turn is followed by an increase of around ten copies (63.46-63.56 Mb, ≈100 kb). It is unclear if these events are part of the same complex (Sup Fig 4 shows the estimated number of copies in each of the above mentioned CNV regions). Considering only the three CNVs which are part of the complex, the inverted Chromosome 1A is at least 500 kb larger than the reference (i.e. the normal non-inverted) haplotype. However, summing the CNV complex with other upstream CNV regions that are also only present in sequenced inv-norm birds (i.e. a region with ≈100 copies followed by other regions with ≈10 copies), suggests that the inverted chromosome may be up to 3.5 Mb larger than the normal chromosome.

As split reads from sequencing data are useful to reveal complex rearrangements in the genome, we evaluated their pattern in the CNVR. We identified split reads in this region that support a complex genomic rearrangement involving different CNVs. Split reads and discordantly mapped paired reads show that this region contains a complex rearrangement of three intervals

which are arranged in a different order and orientation when compared to the reference genome (supplementary section patterns in split reads supporting the CNV complex, Figure 5).

In addition, Lumpy (Layer et al., 2014) was used to predict the exact breakpoints of the inversion. We were unable to infer the whole inversion event from sequencing data, but interestingly one large inversion was unique to the two inv-norm samples that were sequenced. The inversion boundaries are from 62.15 to 63.55 Mb, with a length of 1.4 Mb on the reference genome. For the two inv-norm samples, 9 (sample name = 233) and 8 (sample name = 973) reads supported this 1.4 Mb inversion event. The coordinates of the inversion start lies within a single copy region, while the coordinates of the inversion end are located in the CNV complex (65.87-67.65 Mb). Therefore, we hypothesize that at least one of the inversion breakpoints is within the large complex; however, the precise coordinates are difficult to predict.

Gene content and functionality at the inversion breakpoint. Genomic regions around the inversion breakpoints can have a different structure and nucleotide diversity compared to the rest of the inversion (Andolfatto et al., 2001; Branca et al., 2011; Hoffmann and Rieseberg, 2008). The CNV complex overlaps 32 genes associated with a broad range of phenotypes in other species (for details on the phenotypes associated with each gene see supplementary section 3.3 Genes overlapping the CNVR at the CNV complex). It is perhaps noteworthy that three genes (*BPGM*, *CALD1* and *PIK3C2G*) could potentially be broken in the inverted haplotype, given that sequencing data shows CNVs only partially overlapping them.

Discussion

Here we have described a large putative inversion on Chromosome 1A of the great tit (Bosse et al., 2017) that covers more than 90% of the chromosome and contains almost 1,000 genes. The inversion is present in 5% of the analyzed Dutch population as well as in two out of 29 resequenced individuals from other European populations; one carrier was from Belgium and the other from France, indicating that the inversion is present in other great tit populations as well. In this study, the inversion was analyzed with a SNP array and by shotgun sequencing. Although the most likely explanation for suppressed recombination is an inversion (Kirkpatrick, 2010), we acknowledge that methods such as FISH (Bishop, 2010) and long read sequencing (Shao et al., 2018) need to be used to confirm the inversion hypothesis. It is feasible, though unlikely given the size of the region, that suppressed recombination leading to chromosomal divergence could arise without a chromosomal inversion (Bergero et al., 2008, 2007, 2013; Natri et al., 2013). For clarity in this discussion we refer to the putative inversion found here simply as inversion.

In the population from the Netherlands, among the 2,296 birds analyzed after filtering, no homozygous bird for the inversion on Chromosome 1A was found. Given that very large inversions can cause homozygous lethality in songbirds (Tuttle et al., 2016), we investigated if this great tit population has significantly fewer homozygous inverted birds than expected. However, given the low frequency of the inversion, and assuming Hardy-Weinberg Equilibrium, we would expect less than two homozygous inverted birds and it is thus unclear whether the complete absence of homozygotes is due to a deleterious recessive effect of the inversion or

whether homozygotes are present in the population but not sampled in this study. A possible lethal effect of this inversion could be tested by exploring the frequency of genotypes among offspring of mated carriers. Given the structural complexity and large size of this inversion, a relevant biological effect could be expected. A CNV complex located at the downstream breakpoint encloses 32 genes involved in a wide range of biological processes, which could significantly change the amounts of the transcripts/proteins due to copy number changes in the genes located at the CNV complex. Future studies of this inversion polymorphism will be directed to test the lethality hypothesis and to measure the relative fitness of wildtype homozygotes, inversion carriers and inversion homozygotes. Indeed, this future goal was one motivation for developing a cheap and quick method (based on PCR-RFLP) to more easily type inversion karyotypes.

To identify the inversion without SNP array data, we selected the SNP with highest F_{ST} value that concomitantly would produce a PCR-RFLP profile capable of distinguishing between inversion carriers and non-carries. The selected SNP is located at the first intron of the *PIK3C2G* gene, which is within the CNV complex at one of the putative inversion breakpoints. Along with *PIK3C2G*, several other genes are also located in the CNV complex and these genes have crucial roles in a broad range of processes from cell cycle to gene silencing (supplementary section 3.3 Genes overlapping the CNVR at the CNV complex). Resequenced birds showed a high number of copies within that genomic region ($\approx$10 copies in two inv-norm birds). Moreover, the PCR-RFLP gel intensities support at least four genotypes (three for norm-norm and one for inv-norm birds). Thus, this substantial copy number change in inv-norm birds could underlie

distinct patterns in gene expression and consequently phenotypic variation. Interestingly, such complex rearrangements at inversion breakpoints have a key evolutionary roles in other species e.g. an effect on malaria vectorial capacity in mosquitoes (Sharakhov et al., 2006).

A CNV complex located at the breakpoint seems to be older than the inversion. Assuming a single origin for this complex, the CNV sequences may be older than the inversion given that it is present in virtually all inv-norm birds whereas it occurs at low frequency in norm-norm birds. More than 10% of the norm-norm birds have at least one CNV overlapping the CNV complex. In addition, a repetitive structure is usually found at inversion breakpoints underlying their mechanisms of formation (such as non-allelic homologous recombination - NAHR, Carvalho and Lupski (2016); Hoffmann and Rieseberg (2008)). Thus, it is possible that the inversion is a result of the CNV sequences, which underpinned the mechanism of the inversion formation. However it remains possible that CNVs are present in the inversion only due to a hitchhiking effect and thus did not necessarily contribute to the inversions formation. The hypothesis that CNVs might have underpinned the formation of the inversion remains speculative and needs further investigation. Considering the size of all CNVs associated with the inversion (i.e. complex with ≈10 copies and another complex of ≈10 copies with an additional region with ≈100 copies, identified by sequencing) the inverted chromosome is estimated to be approximately 3.5 Mb larger than the reference sequence reported in genome build 1.1. The greater length of chromosomes harboring the inversion is in line with the hypothesis of degenerative expansion in young supergenes (Stolle et al., 2018). However, genetic variation is not only present in the CNV complex but also at the center of the inversion.

Allele phasing in inv-norm birds is challenging because phasing strategies like BEAGLE assume Hardy-Weinberg equilibrium Browning and Browning (2007); this assumption is often violated at inversion genotype-informative SNPs (i.e the vast majority of the genotype-informative SNPs significantly deviate from HWE). Thus, we used the genotype distribution (i.e. the proportions of "AA", "AB" and "BB" genotypes) to partially explore the haplotypes in the inversion. There are at least two (and perhaps three or more) putative inversion haplotypes, which are reflected by the number of AA genotypes at the center of the inversion (located at ≈20-55 Mb of the Chromosome 1A, Figure 3, note the log scale and three distinct groups). In the LD analysis, only the R^2 metric reflected the variation within inv-norm birds. This variation derives from the SNPs that are located in the center of the inversion (i.e. LD block in the center, Figure 2c and d). The R^2 method has a constraint to deal with low frequency alleles (Wray, 2005) whereas D' is not highly dependent upon allelic frequencies (Hedrick, 1987). Interestingly, in the inv-norm population, the frequency of the less common genotype in the informative SNPs at the R^2 LD block (Figure 2a) is not as low as in the rest of the inversion (Figure 2b). Thus, the distribution of allele frequencies in the inv-norm birds may explain why the R^2 metric does not describe elevated LD, outside the center of the inversion, and is consistent with the hypothesis of a higher recombination rate in the center. In other words, because the two different LD measures are not equally sensitive to rare alleles, and because the allele frequencies seem to be different in the center of the inversion than elsewhere, one metric finds a pattern that the other misses. Presumably this is because occasional recombination has caused allele frequencies and LD patterns to be slightly different in the center than in the rest of the inversion.

Due to the expected very low rates of recombination within the inversion in heterozygotes (Kirkpatrick, 2010), we did not expect multiple haplotypes for the inversion. However, on timescales of 10^5 generations or longer, even this limited recombination works as an important source of variation within inversions (Kirkpatrick, 2010). Indeed, gene conversion and multiple crossing overs, at least far from the breakpoints, are possible within inversions (Andolfatto et al., 2001; Hoffmann and Rieseberg, 2008; Korunes and Noor, 2018). Thus, rare recombination events may explain distinct haplotypes found in the center of the inversion. Moreover, as CNVs can underlie mechanisms of formation and be prone to errors, independent inversion events and errors during meiosis cannot be discarded.

It is unclear whether the inversion has any phenotypic effects. Nevertheless, the CNVs identified by sequencing at the CNV complex directly overlap at least three genes, including *CALD1* involved in smooth muscle contraction (Walsh, 1994), *BPGM* underlying oxygen sensing in blood cells (Petousi et al., 2014) and the above mentioned *PIK3C2G* gene (the other 29 genes overlap a CNVR in the same region but do not overlap partially CNVs identified by sequencing). On other songbird species, such as the zebra finch (*Taeniopygia guttata*), sperm morphology and motility is associated with an inversion in the Z Chromosome (Kim et al., 2017). Moreover, inversions in zebra finches can have strong additive effects on several morphological traits and increase mortality rates (Knief et al., 2016). In white-throated sparrows, which display different plumage morphs and sexual behavior, a large inversion involving up to 1,000 genes and lethal in its homozygous state, has a profound role in disassortative mating (Tuttle et al., 2016). However, there is no evidence of distinct morphs in great tit. Thus, if the inversion is underlying any kind of

mate choice it may be reflected by a more subtle trait or behaviour. Apart from songbirds, large inversions can underlie a number of phenotypes in nature, ranging from mimicry and crypsis in butterflies and moths (Nadeau et al., 2016) to meiotic drive in mice (Lyon, 2003). Our detailed characterization of the variability and complexity of this large inversion provides the foundation for further studies aiming to discover the phenotypic effects and the evolutionary role of this inversion.

Competing Financial Interests None.

Data deposition The raw genotype datasets used during the current study are available at NCBI (https://www.ncbi.nlm.nih.gov/geo/query/acc.cgi?acc=GSE105131).

Acknowledgements VHS benefited of a joint grant from the European Commission within the framework of the Erasmus-Mundus joint doctorate "EGS-ABG". Part of this work was funded by an ERC Advanced Grant (339092 - E-Response) to MEV.

Ethics approval This work was carried out under a license of the Animal Experimental Committee of the Royal Dutch Academy of Sciences (KNAW) protocol NIOO-10.07.

Figure captions

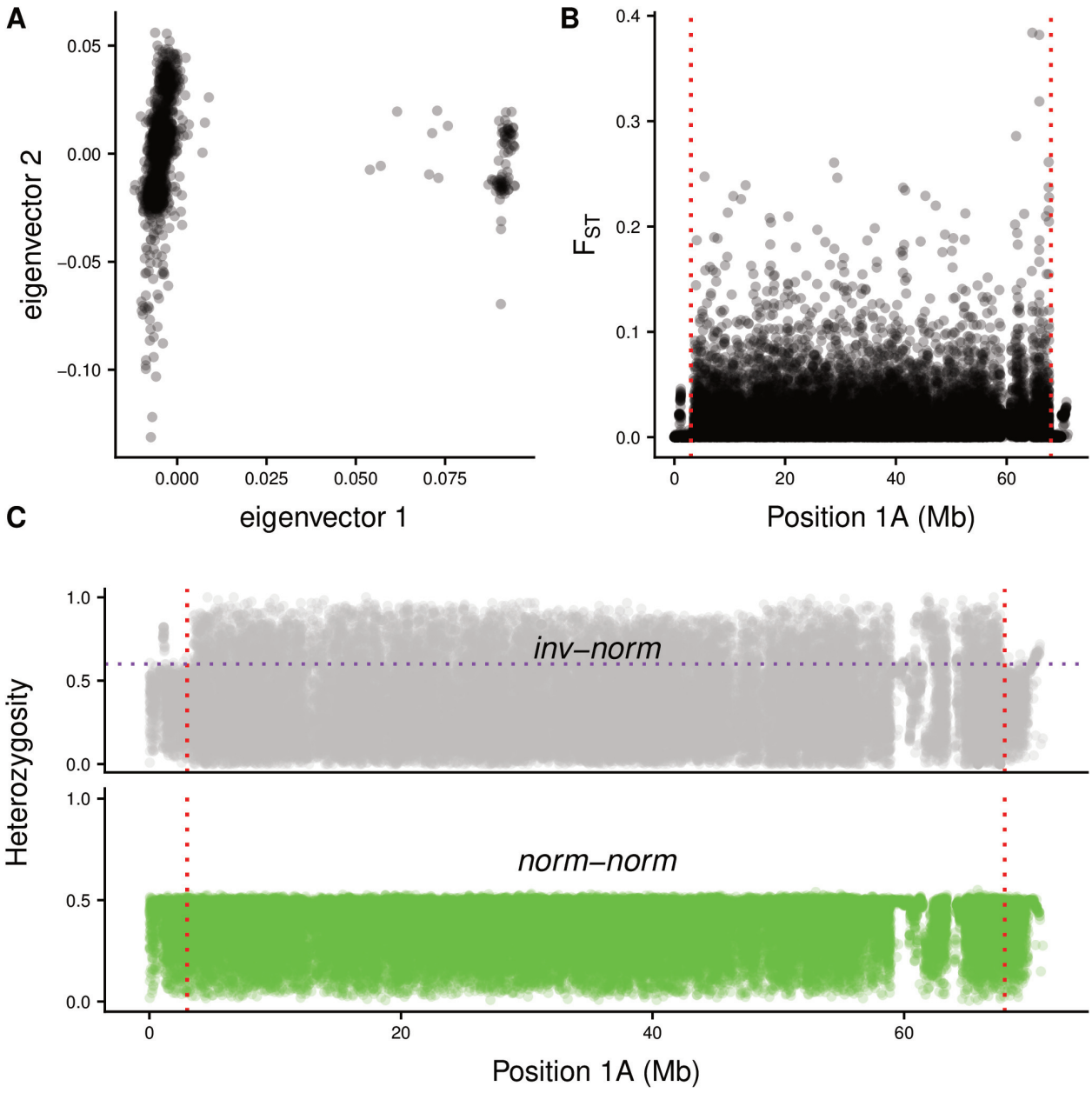

Fig. 1: **A) PCA:** based on the SNPs located on Chromosome 1A, a principal component analysis revealed two distinct subpopulations. The distinction is given by Eigenvector One, which gave the initial evidence of inversion carriers. **B)** F_{ST}**:** these two subpopulations display highly differentiated SNPs across the whole of Chromosome 1A, except at regions near to telomeres. **C) Heterozygosity:** each subpopulation exhibits a particular heterozygosity level across the Chromosome 1A. The inv-norm subpopulation has many SNPs with high heterozygosity within the region bounded by the tentative breakpoints given by F_{ST} analysis (≈3 to 68 Mb, delimited by the red dashed lines). The purple dashed line represents the maximum expected in norm-norm birds. SNPs above this threshold are considered informative.

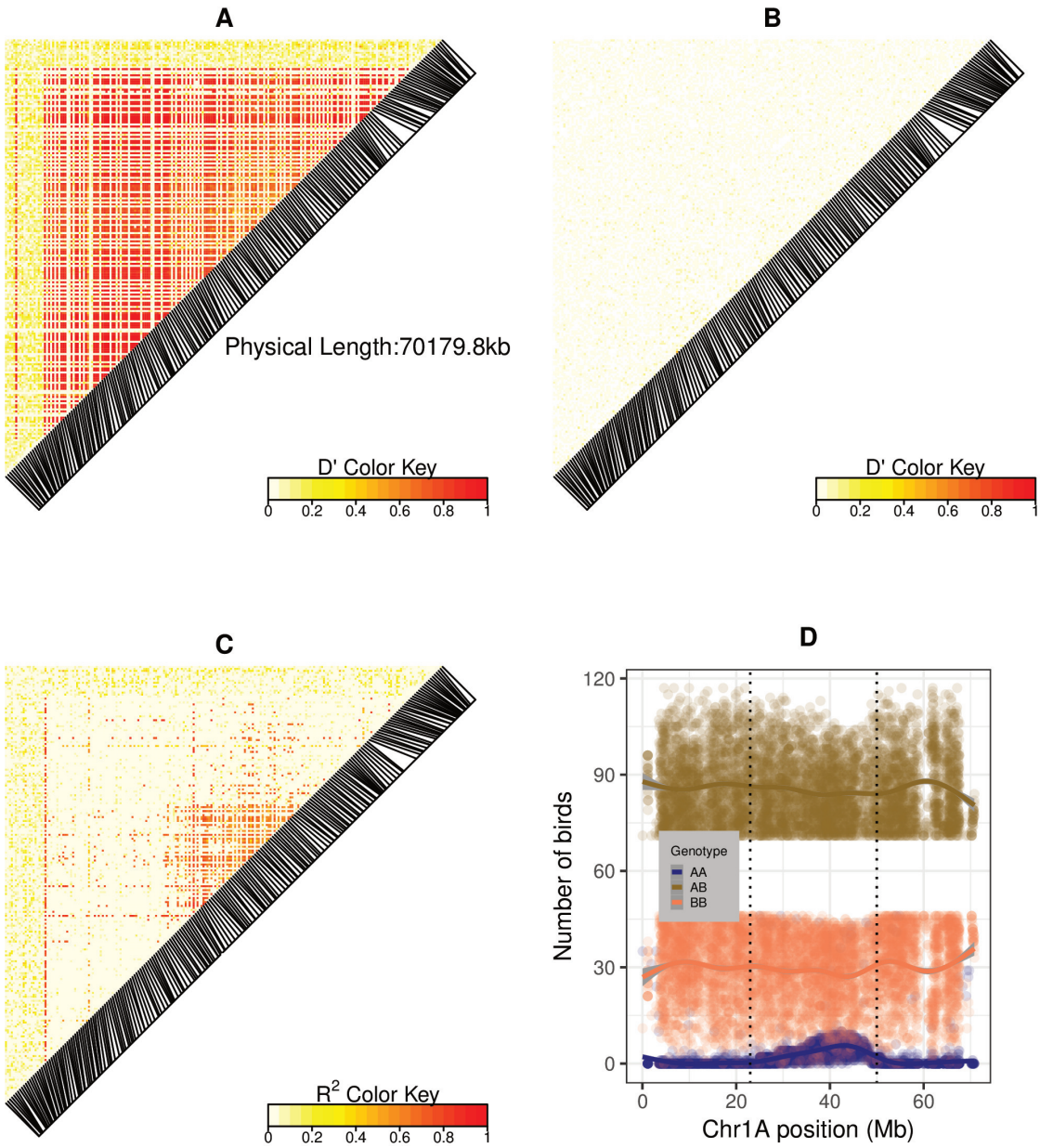

Fig. 2: **The pairwise linkage-disequilibrium on the Chromosome 1A. A)** D' measured in 2,296 great tits. **B)** D' measured in 2,179 norm-norm birds. Figures in the lower panels (C and D) support possible recombination events in the center of the inversion. In other words, possible recombination in the center of the inversion is supported by the distinct genotype distribution in comparison with the rest of the inversion and confirmed by R^2. As R^2 metric has reduced power to detect LD among SNPs with low allele frequency, the LD is reflected only in the center of the inversion. **C)** R^2 measured in 2,296 great tits reveals an LD block only in the middle of the chromosome. The full inversion does not show elevated LD, due to the limitation of R^2 at dealing with low frequency SNP alleles outside the center of the inversion. **D)** Genotype frequency of informative SNPs (heterozygosity > 0.6) across Chromosome 1A in the inv-norm subpopulation. The vertical dotted line roughly indicates the genomic region of middle block which harbors a higher number of birds with "AA" genotypes when compared to the rest of the inversion. Along with the LD pattern from R^2 method, the genotype frequencies suggest a different genetic structure at the center of the inversion.

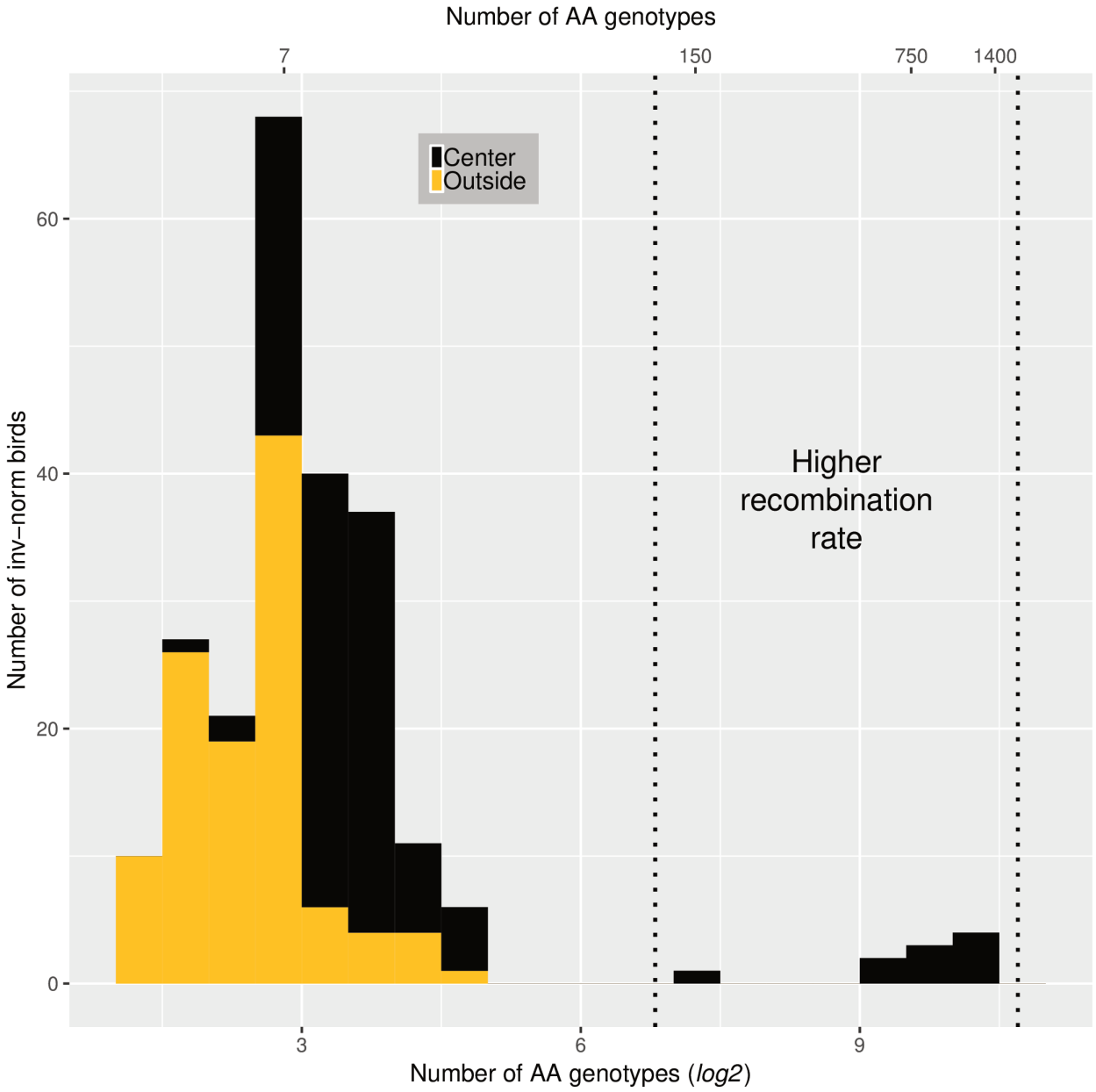

Fig. 3: **Genotype distribution within/outside the center of the inversion (20-55 Mb) in inversion carriers.** The number of genotypes is represented on a log_2 scale to improve the visualization but untransformed values are shown on the upper x-axis. Based on the number of "AA"genotypes it is possible to identify inv-birds birds which harbour a different genotype distribution at the center of the inversion and therefore possibly have different inversion haplotypes (black bars among the dashed lines).

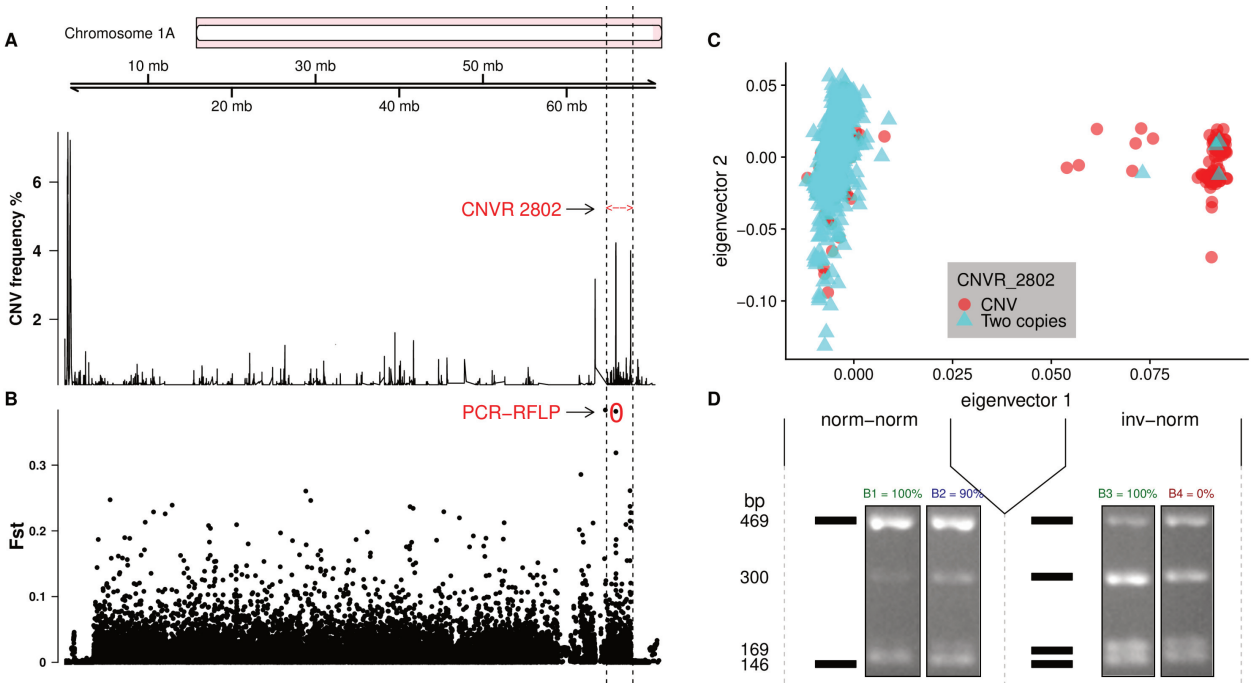

Fig. 4: **CNVs in the inversion breakpoint. A)** CNV frequency across the Chromosome 1A and the genomic interval of the previously identified CNV region '2802' (≈64.83-67.67 Mb, da Silva et al. (2018)), which is located at the inversion breakpoint. **B)** F_{ST} values across the chromosome. A red circle is highlighting the SNP used to the PCR-RFLP analysis. **C)** A CNV in the inversion breakpoint is present in the vast majority of inv-norm birds whereas is rarely found in norm-norm birds. **D)** Digestion pattern of the PCR-RFLP at the SNP AX-100689781. The black bars represent the expected gel patterns alongside each of the two observed patterns in each subpopulation (i.e. norm-norm and inv-norm). Distinct copy number genotypes are evidenced by the allele intensities in the gel after electrophoresis. The values above each gel picture depicts the fingerprint name and the degree of confidence to tag a specific karyotype state (i.e. percent of the birds with concordant inversion genotype between SNP array and PCR-RFLP). Green was used in highly confident profiles, blue in the medium confidence one and red for B4, which has high heterozygosity (expected in inv-norm) but was only identified in two norm-norm birds. To differentiate between fingerprints note the distinct intensities of subsets of bands; between B1 and B2 the greatest difference is mainly at the 300/169 bp bands and between B3 and B4 the greatest difference is between the 469/300 bp bands.

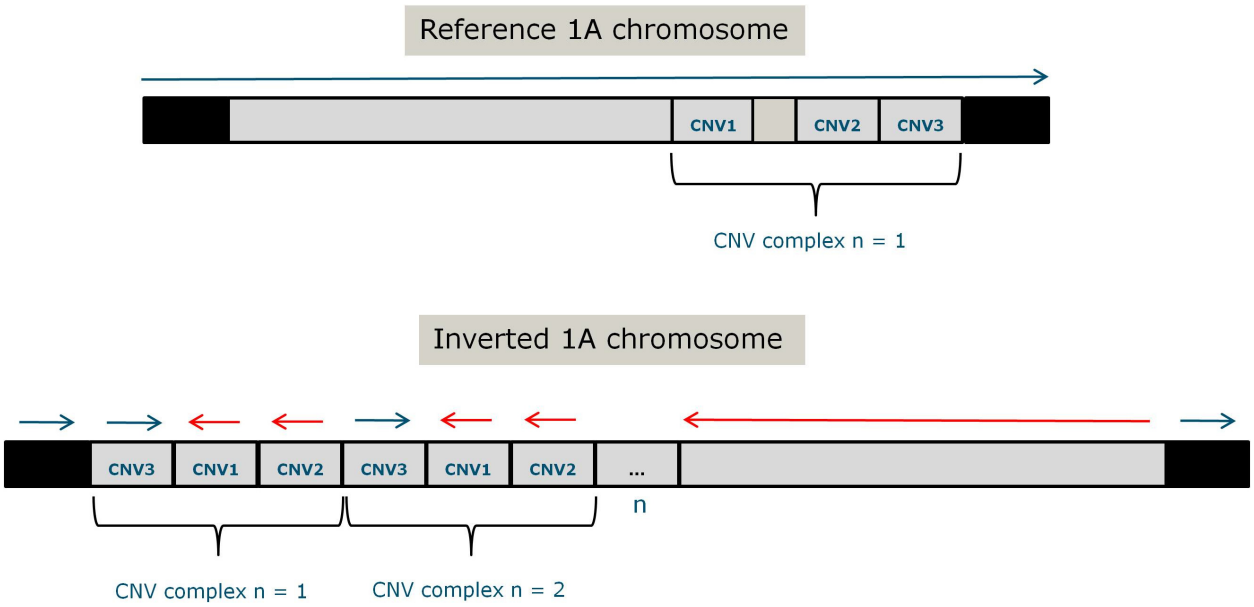

Fig. 5: **Representation of the whole Chromosome 1A with the complex structural rearrangement in the downstream breakpoint of the inversion.** Blocks in grey represent the inversion region whereas those in black are genomic regions outside the inversion. CNVs identified by sequencing in the two inv-norm birds which were sequenced are labeled as CNV1-3 for simplicity. Horizontal curly brackets define the structural complex which encompasses CNVs 1-3. The above chromosomal representation displays the chromosome as shown in the reference genome (Laine et al., 2016). The below representation displays the expected genomic structure in the inversion. CNVs are relatively larger than their real length for schematic purposes.

References

Andolfatto P, Depaulis F, Navarro A. 2001, feb. Inversion polymorphisms and nucleotide variability in Drosophila. Genet. Res. (Camb). 77(01).

Bergero R, Charlesworth D, Filatov DA, Moore RC. 2008, apr. Defining Regions and Rearrangements of the Silene latifolia Y Chromosome. Genetics. 178(4):2045–2053.

Bergero R, Forrest A, Kamau E, Charlesworth D. 2007, feb. Evolutionary Strata on the X Chromosomes of the Dioecious Plant Silene latifolia: Evidence From New Sex-Linked Genes. Genetics. 175(4):1945–1954.

Bergero R, Qiu S, Forrest A, Borthwick H, Charlesworth D. 2013, jul. Expansion of the Pseudo-autosomal Region and Ongoing Recombination Suppression in the Silene latifolia Sex Chromosomes. Genetics. 194(3):673–686.

Bishop R. 2010, mar. Applications of fluorescence in situ hybridization (FISH) in detecting genetic aberrations of medical significance. Bioscience Horizons. 3(1):85–95.

Bosse M, Spurgin LG, Laine VN, Cole EF, Firth JA, et al. 2017, oct. Recent natural selection causes adaptive evolution of an avian polygenic trait. Science. 358(6361):365–368.

Branca A, Paape TD, Zhou P, Briskine R, Farmer AD, et al. 2011, sep. Whole-genome nucleotide diversity, recombination, and linkage disequilibrium in the model legume medicago truncatula. Proceedings of the National Academy of Sciences. 108(42):E864–E870.

Browning SR, Browning BL. 2007, nov. Rapid and Accurate Haplotype Phasing and Missing-Data Inference for Whole-Genome Association Studies By Use of Localized Haplotype Clustering. Am. J. Hum. Genet. 81(5):1084–1097.

Butlin RK. 2005, aug. Recombination and speciation. Molecular Ecology. 14(9):2621–2635.

Calvete O, Gonzalez J, Betran E, Ruiz A. 2012, jul. Segmental Duplication, Microinversion, and Gene Loss Associated with a Complex Inversion Breakpoint Region in Drosophila. Mol. Biol. Evol. 29(7):1875–1889.

Carvalho CMB, Lupski JR. 2016, feb. Mechanisms underlying structural variant formation in genomic disorders. Nat. Rev. Genet. 17(4):224–238.

Chiang C, Layer RM, Faust GG, Lindberg MR, Rose DB, et al. 2015, aug. SpeedSeq: ultra-fast personal genome analysis and interpretation. Nat. Methods. 12(10):966–968.

Clayton D. 2015. snpStats: SnpMatrix and XSnpMatrix classes and methods.

da Silva VH, Laine VN, Bosse M, van Oers K, Dibbits B, et al. 2018, mar. CNVs are associated with genomic architecture in a songbird. BMC Genomics. 19(S2):195.

Excoffier L, Slatkin M. 1995, sep. Maximum-likelihood estimation of molecular haplotype frequencies in a diploid population. Mol. Biol. Evol. 12(5):921–7.

Furuta Y, Kawai M, Yahara K, Takahashi N, Handa N, et al. 2011, jan. Birth and death of genes linked to chromosomal inversion. Proc. Natl. Acad. Sci. 108(4):1501–1506.

Geistlinger L, da Silva VH, Cesar ASM, Tizioto PC, Waldron L, et al. 2018, dec. Widespread modulation of gene expression by copy number variation in skeletal muscle. Scientific Reports. 8(1):1399.

Hedrick PW. 1987, oct. Gametic disequilibrium measures: proceed with caution. Genetics. 117(2):331–41.

Hellen EH. 2015, nov. Inversions and Evolution of the Human Genome. In: eLS. John Wiley & Sons, Ltd. p. 1–6.

Hoffmann AA, Rieseberg LH. 2008, dec. Revisiting the Impact of Inversions in Evolution: From Population Genetic Markers to Drivers of Adaptive Shifts and Speciation? Annu. Rev. Ecol. Evol. Syst. 39(1):21–42.

Hooper DM, Price TD. 2017, oct. Chromosomal inversion differences correlate with range overlap in passerine birds. Nat. Ecol. Evol. 1(10):1526–1534.

Huang YC, Dang VD, Chang NC, Wang J. 2018, may. Multiple large inversions and breakpoint rewiring of gene expression in the evolution of the fire ant social supergene. Proceedings of the Royal Society B: Biological Sciences. 285(1878):20180221.

Husby A, Visser ME, Kruuk LEB. 2011. Speeding Up Microevolution: The Effects of Increasing Temperature on Selection and Genetic Variance in a Wild Bird Population. PLoS Biol. 9(2):e1000585.

Kehrer-Sawatzki H, Cooper DN. 2008, mar. Molecular mechanisms of chromosomal rearrangement during primate evolution. Chromosom. Res. 16(1):41–56.

Keller L, Ross KG. 1998, aug. Selfish genes: a green beard in the red fire ant. Nature. 394(6693):573–575.

Kim JM, Santure AW, Barton HJ, Quinn JL, Cole EF, et al. 2018, jul. A high-density SNP chip for genotyping great tit (Parus major) populations and its application to studying the genetic architecture of exploration behaviour. Molecular Ecology Resources. 18(4):877–891.

Kim KW, Bennison C, Hemmings N, Brookes L, Hurley LL, et al. 2017, aug. A sex-linked supergene controls sperm morphology and swimming speed in a songbird. Nat. Ecol. Evol. 1(8):1168–1176.

Kirkpatrick M. 2006, mar. Chromosome Inversions, Local Adaptation and Speciation. Genetics. 173(1):419–434.

Kirkpatrick M. 2010, sep. How and Why Chromosome Inversions Evolve. PLoS Biol. 8(9):e1000501.

Knief U, Hemmrich-Stanisak G, Wittig M, Franke A, Griffith SC, et al. 2016, dec. Fitness consequences of polymorphic inversions in the zebra finch genome. Genome Biology. 17(1):199.

Korunes KL, Noor MAF. 2018, dec. Pervasive gene conversion in chromosomal inversion heterozygotes. Molecular Ecology.:mec.14921.

Küpper C, Stocks M, Risse JE, dos Remedios N, Farrell LL, et al. 2015, nov. A supergene determines highly divergent male reproductive morphs in the ruff. Nat. Genet. 48(1):79–83.

Kvist L, Martens J, Higuchi H, Nazarenko AA, Valchuk OP, et al. 2003, jul. Evolution and genetic structure of the great tit (Parus major) complex. Proc. R. Soc. B Biol. Sci. 270(1523):1447–1454.

Laine VN, Gossmann TI, Schachtschneider KM, Garroway CJ, Madsen O, et al. 2016, jan. Evolutionary signals of selection on cognition from the great tit genome and methylome. Nat. Commun. 7:10474.

Lamichhaney S, Fan G, Widemo F, Gunnarsson U, Thalmann DS, et al. 2016, jan. Structural genomic changes underlie alternative reproductive strategies in the ruff (Philomachus pugnax). Nature Genetics. 48(1):84–88.

Layer RM, Chiang C, Quinlan AR, Hall IM. 2014. LUMPY: a probabilistic framework for structural variant discovery. Genome Biol. 15(6):R84.

Lewontin RC. 1964, jan. The Interaction of Selection and Linkage. I. General Considerations; Heterotic Models. Genetics. 49(1):49–67.

Lewontin RC, Kojima Ki. 1960, dec. The Evolutionary Dynamics of Complex Polymorphisms. Evolution (N. Y). 14(4):458.

Li H, Durbin R. 2009, jul. Fast and accurate short read alignment with Burrows-Wheeler transform. Bioinformatics. 25(14):1754–1760.

Li H, Handsaker B, Wysoker A, Fennell T, Ruan J, et al. 2009, aug. The Sequence Alignment/Map format and SAMtools. Bioinformatics. 25(16):2078–2079.

Lucas C, Nicolas M, Keller L. 2015, feb. Expression of foraging and Gp-9 are associated with social organization in the fire ant Solenopsis invicta. Insect Mol. Biol. 24(1):93–104.

Lyon MF. 2003, dec. Transmission Ratio Distortion in Mice. Annual Review of Genetics. 37(1):393–408.

Ma J, Amos CI. 2012, jul. Investigation of Inversion Polymorphisms in the Human Genome Using Principal Components Analysis. PLoS One. 7(7):e40224.

McGaugh SE, Heil CSS, Manzano-Winkler B, Loewe L, Goldstein S, et al. 2012, nov. Recombination Modulates How Selection Affects Linked Sites in Drosophila. PLoS Biol. 10(11):e1001422.

Nadeau NJ, Pardo-Diaz C, Whibley A, Supple MA, Saenko SV, et al. 2016, jun. The gene cortex controls mimicry and crypsis in butterflies and moths. Nature. 534(7605):106–110.

Natri HM, Shikano T, Merilä J. 2013, may. Progressive Recombination Suppression and Differentiation in Recently Evolved Neo-sex Chromosomes. Molecular Biology and Evolution. 30(5):1131–1144.

Nicolazzi EL, Iamartino D, Williams JL. 2014, nov. AffyPipe: an open-source pipeline for Affymetrix Axiom genotyping workflow. Bioinformatics. 30(21):3118–3119.

Nipitwattanaphon M, Wang J, Dijkstra MB, Keller L. 2013, jul. A simple genetic basis for complex social behaviour mediates widespread gene expression differences. Molecular Ecology. 22(14):3797–3813.

Patterson N, Price AL, Reich D. 2006, dec. Population structure and eigenanalysis. PLoS Genet. 2(12):e190.

Petousi N, Copley RR, Lappin TRJ, Haggan SE, Bento CM, et al. 2014, oct. Erythrocytosis associated with a novel missense mutation in the BPGM gene. Haematologica. 99(10):e201–e204.

Puig M, Caceres M, Ruiz A. 2004, jun. Silencing of a gene adjacent to the breakpoint of a widespread Drosophila inversion by a transposon-induced antisense RNA. Proc. Natl. Acad. Sci. 101(24):9013–9018.

Shao H, Ganesamoorthy D, Duarte T, Cao MD, Hoggart CJ, et al. 2018, dec. npInv: accurate detection and genotyping of inversions using long read sub-alignment. BMC Bioinformatics. 19(1):261.

Sharakhov IV, White BJ, Sharakhova MV, Kayondo J, Lobo NF, et al. 2006, apr. Breakpoint structure reveals the unique origin of an interspecific chromosomal inversion (2La) in the Anopheles gambiae complex. Proc. Natl. Acad. Sci. 103(16):6258–6262.

Shin JH, Blay S, McNeney B, Graham J. 2006. Ldheatmap: An r function for graphical display of pairwise linkage disequilibria between single nucleotide polymorphisms. J Stat Soft. 16.

Stevison LS, Hoehn KB, Noor MAF. 2011, sep. Effects of Inversions on Within- and Between-Species Recombination and Divergence. Genome Biol. Evol. 3:830–841.

Stolle E, Pracana R, Howard P, Paris CI, Brown SJ, et al. 2018, dec. Degenerative expansion of a young supergene. Molecular Biology and Evolution.

Thompson MJ, Jiggins CD. 2014, jul. Supergenes and their role in evolution. Heredity. 113(1):1–8.

Tuttle EM, Bergland AO, Korody ML, Brewer MS, Newhouse DJ, et al. 2016, feb. Divergence and Functional Degradation of a Sex Chromosome-like Supergene. Curr. Biol. 26(3):344–350.

Visser ME, Noordwijk AJv, Tinbergen JM, Lessells CM. 1998, oct. Warmer springs lead to mistimed reproduction in great tits (Parus major). Proc. R. Soc. B Biol. Sci. 265(1408):1867–1870.

Walsh MP. 1994, jun. Calmodulin and the regulation of smooth muscle contraction. Mol. Cell. Biochem. 135(1):21–41.

Wang J, Ross KG, Keller L. 2008, jul. Genome-Wide Expression Patterns and the Genetic Architecture of a Fundamental Social Trait. PLoS Genetics. 4(7):e1000127.

Wang J, Wurm Y, Nipitwattanaphon M, Riba-Grognuz O, Huang YC, et al. 2013, jan. A Y-like social chromosome causes alternative colony organization in fire ants. Nature. 493(7434):664–668.

Wray NR. 2005, apr. Allele Frequencies and the r2 Measure of Linkage Disequilibrium: Impact on Design and Interpretation of Association Studies. Twin Res. Hum. Genet. 8(02):87–94.

Xie C, Tammi MT. 2009*a*. CNV-seq, a new method to detect copy number variation using high-throughput sequencing. BMC Bioinformatics. 10(1):80.

Xie C, Tammi MT. 2009*b*. CNV-seq, a new method to detect copy number variation using high-throughput sequencing. BMC Bioinformatics. 10(1):80.

Zaykin DV, Pudovkin A, Weir BS. 2008, aug. Correlation-Based Inference for Linkage Disequilibrium With Multiple Alleles. Genetics. 180(1):533–545.

Zheng X, Levine D, Shen J, Gogarten SM, Laurie C, et al. 2012, dec. A high-performance computing toolset for relatedness and principal component analysis of SNP data. Bioinformatics. 28(24):3326–3328.